Inorg. Chem. **2005**, *44*, 4852–4861

Aqueous Reductive Dechlorination of Chlorinated Ethylenes with Tetrakis(4-carboxyphenyl)porphyrin Cobalt

Joseph M. Fritsch and Kristopher McNeill*

Department of Chemistry, University of Minnesota, 225 Pleasant Street SE, Minneapolis, Minnesota 55455

Received March 23, 2005

The catalytic dechlorination of chlorinated ethylenes by 5,10,15,20-tetrakis(4-carboxyphenyl)porphyrin cobalt ((TCPP)-Co), a cobalt complex structurally similar to vitamin B_{12}, was studied. It was found to have superior aqueous-phase dechlorination activity on chlorinated ethylenes (CEs) relative to vitamin B_{12}. Bimolecular rate constants for the degradation of CEs by (TCPP)Co of 250, 24, 0.24, and 1.5 M^{-1} s^{-1} were found for perchloroethylene (PCE), trichloroethylene (TCE), *cis*-dichloroethylene (cDCE), and *trans*-dichloroethylene (tDCE), respectively. Through kinetic analysis, the rate laws for PCE and TCE were determined to be first order in substrate and catalyst, and PCE degradation was shown to be sensitive to the concentration of the titanium citrate bulk reductant and pH. The importance of the Co^{I} oxidation state on dehalogenation was studied with UV–vis absorbance spectroscopy, a variety of reducing agents, and cyclic voltammetry. Evidence of chlorovinyl complexes as potential catalytic cycle intermediates was obtained through the preparation of (TPP)Co(*trans*-C_2H_2Cl) and the observation of (TPP)Co-(C_2HCl_2) and (TCPP)Co(C_2HCl_2) by mass spectrometry. The X-ray crystal structure of (TPP)Co(*trans*-C_2H_2Cl) is reported.

Introduction

Chlorinated ethylenes (CEs), specifically perchloroethylene (PCE) and trichloroethylene (TCE), are widespread groundwater pollutants listed as United States Environmental Protection Agency priority pollutants.[1−3] Many studies have been undertaken aimed at the dechlorination of these compounds by zero-valent metals,[4−6] electrochemical processes,[7−10] and microbial approaches.[11,12] Dechlorination catalysis involving vitamin B_{12} has attracted interest because of its involvement in natural systems, potential in remediation, and diverse mechanisms utilized for degradation of different CE substrates (including outer-sphere electron transfer, inner-sphere electron transfer, and cobalt−carbon bond formation) (Scheme 1).[13−23]

* To whom correspondence should be addressed. E-mail: mcneill@chem.umn.edu.

(1) Doherty, R. E. *Environ. Forensics* **2000**, *1*, 83−93.
(2) Doherty, R. E. *Environ. Forensics* **2000**, *1*, 69−81.
(3) Squillace, P. J.; Moran, M. J.; Lapham, W. W.; Price, C. V.; Clawges, R. M.; Zogorski, J. S. *Environ. Sci. Technol.* **1999**, *33*, 4176−4187.
(4) Roberts, A. L.; Totten, L. A.; Arnold, W. A.; Burris, D. R.; Campbell, T. J. *Environ. Sci. Technol.* **1996**, *30*, 2654−2659.
(5) Arnold, W. A.; Roberts, A. L. *Environ. Sci. Technol.* **1998**, *32*, 3017−3025.
(6) Arnold, W. A.; Roberts, A. L. *Environ. Sci. Technol.* **2000**, *34*, 1794−1805.
(7) Li, T.; Farrell, J. *Environ. Sci. Technol.* **2001**, *35*, 3560−3565.
(8) Li, T.; Farrell, J. *Environ. Sci. Technol.* **2000**, *34*, 173−179.
(9) Lowry, G. V.; Reinhard, M. *Environ. Sci. Technol.* **1999**, *33*, 1905−1910.
(10) Lowry, G. V.; Reinhard, M. *Environ. Sci. Technol.* **2001**, *35*, 696−702.
(11) Mohn, W. W.; Tiedje, J. M. *Microbiol. Rev.* **1992**, *56*, 482−507.
(12) Middeldorp, P. J. M.; Luijten, M. L. G. C.; Van De Pas, B. A.; Van Eekert, M. H. A.; Kengen, S. W. M.; Schraa, G.; Stams, A. J. M. *Biorem. J.* **1999**, *3*, 151−169.
(13) Gantzer, C. J.; Wackett, L. P. *Environ. Sci. Technol.* **1991**, *25*, 715−722.
(14) Glod, G.; Angst, W.; Holliger, C.; Schwarzenbach, R. P. *Environ. Sci. Technol.* **1997**, *31*, 253−260.
(15) Glod, G.; Brodmann, U.; Angst, W.; Holliger, C.; Schwarzenbach, R. P. *Environ. Sci. Technol.* **1997**, *31*, 3154−3160.
(16) Burris, D. R.; Delcomyn, C. A.; Deng, B.; Buck, L. E.; Hatfield, K. *Environ. Toxicol. Chem.* **1998**, *17*, 1681−1688.
(17) Burris, D. R.; Delcomyn, C. A.; Smith, M. H.; Roberts, A. L. *Environ. Sci. Technol.* **1996**, *30*, 3047−3052.
(18) Schwarzenbach, R. P.; Angst, W.; Holliger, C.; Hug, S. J.; Klausen, J. *Chimia* **1997**, *51*, 908−914.
(19) Semadeni, M.; Chiu, P.-C.; Reinhard, M. *Environ. Sci. Technol.* **1998**, *32*, 1207−1213.
(20) Shey, J.; van der Donk, W. A. *J. Am. Chem. Soc.* **2000**, *122*, 12403−12404.
(21) McCauley, K. M.; Wilson, S. R.; van der Donk, W. A. *Inorg. Chem.* **2002**, *41*, 5844−5848.
(22) McCauley, K. M.; Wilson, S. R.; van der Donk, W. A. *J. Am. Chem. Soc.* **2003**, *125*, 4410−4411.
(23) McCauley, K. M.; Wilson, S. R.; van der Donk, W. A. *Inorg. Chem.* **2002**, *41*, 393−404.

10.1021/ic0504339 CCC: $30.25
Published on Web 05/27/2005

Scheme 1. Partial Perchloroethylene (PCE) Dechlorination Pathway Mediated by Vitamin B_{12}

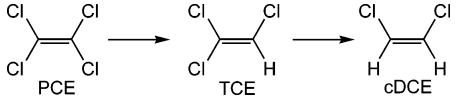

Following a long tradition of modeling B_{12} with simpler cobalt complexes, there have been studies using structurally related cobalt complexes to model intermediates[21−24] and function as catalysts.[25−27] Dror and Schlautmann have recently reported on the PCE dechlorination activity of a broad survey of metalloporphyrins (M = Fe, Co, Ni).[25] Among the findings, catalytic activity was linked to water-soluble porphyrin complexes, including a catalyst precursor tetrakis(4-carboxyphenyl)porphyrin cobalt(II) ((TCPP)Co) that was found to have significant dehalogenation activity against PCE. Vitamin B_{12} and (TCPP)Co have several structural and chemical similarities, including planar tetrapyrrole coordination of cobalt and readily supported common oxidation states of cobalt.[28−31] Because of our interest in the development of synthetic aqueous dehalogenation catalysts, we sought to study the dechlorination chemistry of (TCPP)Co in detail. Here, we report the results of studies designed to establish the kinetic behavior and substrate selectivity of (TCPP)Co with an emphasis on the comparison to structurally similar vitamin B_{12} for which a large amount of mechanistic work has already been performed. This study also features the use of tetraphenylporphyrin cobalt ((TPP)Co) and 5-(4-carboxyphenyl)-10,15,20-tri(phenyl)porphyrin cobalt ((MCPP)Co), which are useful as synthetic models and in probing the importance of the peripheral carboxylates of (TCPP)Co. Through reaction kinetics, spectroscopic and crystallographic studies of intermediates, substrate scope, and product selectivity, we establish that (TCPP)Co is a superb synthetic mimic of B_{12} with superior dechlorination rates.

Experimental Section

Materials. 5,10,15,20-Tetrakis(4-carboxyphenyl)porphyrin cobalt(II) ((TCPP)Co) and 5-(4-carboxyphenyl)-10,15,20-tri(phenyl)-porphyrin cobalt(II) ((MCPP)Co) were purchased from Porphyrin Systems. PCE, TCE, tetraphenylporphyrin cobalt(II) ((TPP)Co), lithium aluminum hydride, chromium(III) chloride, benzophenone, and tris(hydroxymethyl)aminomethane (Tris) were purchased from Aldrich. Cyanocobalamin (vitamin B_{12}) and titanium(III) chloride (30 wt % in 2 N HCl) were purchased from Acros. Tetrabutylammonium hexafluorophosphate ($TBA^+PF_6^-$) was purchased from Fluka. Vinyl chloride (1000 ppm in He) and alkene standards (C_2−C_6, 1000 ppm in He) were purchased from Matheson TriGas via Alltech Associates, Inc. (Deerfield, IL). Acetylene (1.06% in He) was purchased from Scott Specialty Gases via Alltech Associates, Inc. Trisodium citrate monohydrate was purchased from Mallinckrodt. Both *cis*- and *trans*-DCE were purchased from TCI America. Titanium(III) citrate was prepared in a manner similar to a previously published method.[32] Chromous ions were prepared by reduction of $CrCl_3$(aq) with Zn amalgam.[33] Sodium benzophenone ketyl was prepared by the addition of 0.9 equiv of sodium metal to benzophenone in THF.

General Methods. ^{1}H NMR and ^{13}C NMR spectra were determined at 300 and 75 MHz, respectively, on a Varian Inova instrument. ESI-TOF mass spectra were collected on a Bruker BioTOF II instrument. UV−vis absorbance spectra were collected with a Jasco V530 spectrophotometer (300−700 nm) with a 4 mL septum-sealed quartz cuvette. Cyclic voltammograms were collected with a BAS 100B electrochemical analyzer with a normal three-electrode configuration consisting of a highly polished glassy carbon working electrode (A = 0.07 cm^2), a Pt auxiliary electrode, and a Ag/AgCl reference electrode containing 1.0 M KCl.

Kinetic Time Courses. The following instrumentation was used for studies of CE substrate, catalyst, pH, and titanium dependence. Headspace samples (100 μL) were withdrawn and analyzed by splitless injection with a Hewlett-Packard 5890 gas chromatograph, a VOCOL column (30 m × 0.53 mm i.d., 3 μm film thickness, Supelco), and a flame ionization detector. Isothermal temperature programs (PCE 65 °C, TCE 55 °C, and DCEs 35 °C) were used with helium carrier gas (flow = 1 mL/min). Individual CE congeners were identified and quantified by comparison of retention time and peak areas to those of standard samples.

Mass Balance Determination. The following instrumentation was used for determination and quantitation of PCE and TCE degradation products. Headspace samples (100 μL) were analyzed by splitless injection with a ThermoQuest Trace GC, a DB-1 column (30 m × 0.32 mm i.d., 5 μm film thickness, J+W Scientific), and a flame ionization detector. The system was computer controlled with ChromeQuest software as the controller and data storage. The temperature program used was 60 (5 min) → 240 (3.5 min) °C at a rate of 20 °C/min with helium carrier gas (flow = 1 mL/min). Dechlorination products were identified and quantified by comparison of retention time and peak area to those of standard samples. Authentic gas samples were used to quantify the amount of vinyl chloride, acetylene, ethylene, and ethane produced.

X-ray Structure Analysis. Diffraction data on (TPP)Co(*trans*-C_2H_2Cl) mounted on a thin glass capillary with oil were collected on a Siemens SMART Platform CCD diffractometer with Mo Kα radiation (graphite monochromator) at 173(2) K. The structure was solved with direct methods using SHELXS-97 and refined using SHELXL-97.[34] Crystallographic data for (TPP)Co(*trans*-C_2H_2Cl) are given in Table 1. Additional crystallographic data, including tables of bond lengths and angles, are presented in the Supporting Information.

Electrochemistry. Potentials are reported vs aqueous Ag/AgCl and are not corrected for the junction potential. The $E^{\circ\prime}$ values for the ferrocenium/ferrocene couple for concentrations similar to those used in this study were +0.44 V for DMF solutions at a glassy carbon electrode. Cyclic voltammetry (CV) experiments were performed at room temperature (23−24 °C). The 2 mL working compartment was separated from the reference compartment by a

(24) Rich, A. E.; DeGreeff, A. D.; McNeill, K. *Chem. Commun.* **2002**, 234−235.
(25) Dror, I.; Schlautman, M. A. *Environ. Toxicol. Chem.* **2004**, *23*, 252−257.
(26) Marks, T. S.; Allpress, J. D.; Maule, A. *Appl. Environ. Microbiol.* **1989**, *55*, 1258−1261.
(27) Lewis, T. A.; Morra, M. J.; Habdas, J.; Czuchajowski, L.; Brown, P. D. *J. Environ. Qual.* **1995**, *24*, 56−61.
(28) Walker, F. A.; Beroiz, D.; Kadish, K. M. *J. Am. Chem. Soc.* **1976**, *98*, 3484−3489.
(29) Truxillo, L. A.; Davis, D. G. *Anal. Chem.* **1975**, *47*, 2260−2267.
(30) Lexa, D.; Saveant, J. M.; Soufflet, J. P. *J. Electroanal. Chem. Interfacial Electrochem.* **1979**, *100*, 159−172.
(31) Lexa, D.; Lhoste, J. M. *Experientia, Suppl.* **1971**, *No. 18*, 395−405.
(32) Smith, M. H.; Woods, S. L. *Appl. Environ. Microbiol.* **1994**, *60*, 4107−4110.
(33) Dunne, T. G.; Hurst, J. K. *Inorg. Chem.* **1980**, *19*, 1152−1157.
(34) *SHELXTL*, version 6.1; Bruker-AXS: Madison, WI, 2000.

Table 1. Crystal Data and Details of the Structural Refinement for (TPP)Co(*trans*-C_2H_2Cl)

formula	$C_{46}H_{30}ClCoN_4$
fw (g/mol)	733.12
space group	$P2_1/n$
T (K)	173(2)
λ (Å)	0.71073
a (Å)	10.0398(16)
b (Å)	16.148(3)
c (Å)	21.493(3)
α (deg)	90
β (deg)	94.380(3)
γ (deg)	90
ρ_{calcd} (g cm^{-1})	1.402
Z	4
vol (Å^3)	3474.4(10)
μ (cm^{-1})	6.12
R_1,[a] R_2[b] (%) [$I > 2\sigma(I)$]	0.0482, 0.1103
R_1,[a] R_2[b] (%) all data	0.0770, 0.1228

[a] $R_1 = \sum||F_o| - |F_c||/\sum F_o$. [b] $R_2 = [\sum[w(F_o^2 - F_c^2)^2]/\sum w(F_o^2)^2]^{1/2}$.

modified Luggin capillary. All three compartments were filled with a 0.1 M solution of the supporting electrolyte, $TBAPF_6$. The DMF solvent was dried over 4 Å sieves, and the electrolyte and analyte solutions (0.5 mM cobalt porphyrin) were degassed by two freeze−pump−thaw cycles prior to use. The working compartment of the cell was bubbled with argon to deaerate the solution. The electrolyte solution background cyclic voltammograms were collected prior to the analysis of the porphyrin solutions. The electrode was removed from the solution and cleaned to remove any electrode surface aggregates that formed during the electrochemical experiments. The $E^{\circ\prime}$ value for the ferrocenium/ferrocene couple was determined for solutions and concentrations similar to those used in the study of the porphyrin complexes to allow for the correlation of the $E_{p,a}$ and $E_{p,c}$ values to past and future studies. As the peak potentials, in general, depend on the concentration and scan rate, the CV's for the complexes were recorded at similar concentrations (0.5 mM) and scan rates (100 mV/s).

CE Substrate Degradation Kinetic Profiles. The reductive dehalogenation reactions were conducted in 42 mL septum-sealed vials. A stock solution of (TCPP)Co was prepared in DI H_2O with NaOH. The total aqueous reaction volume in the vial was 10 mL. Tris buffer (9 mL of a 110 mM stock solution, pH 8, diluted to 10 mL to give a final concentration of 100 mM) and catalyst (concentrations varied by substrate, for PCE mass balance the catalyst addition was as follows: 250 μL of a 30 μM stock solution diluted to 10 mL to give a final concentration of 750 nM) were added to the vial and deoxygenated by sparging with N_2 for 20 min. The CE stock solution (500 μL of a 1.6 mM PCE and 0.34 mM toluene stock solution diluted to 10 mL to give a final concentration of 80 μM PCE and 17 μM toluene) in methanol was added to the vial. Vials were placed in a 35 °C water bath for 20 min. A time zero data point was collected, and titanium(III) citrate (250 μL of a 640 mM stock solution diluted to 10 mL, final concentration 16 mM) was added to initiate the reaction. The dehalogenation reaction was monitored at regular intervals. Peak areas from CE substrate in the standard and samples were compared to determine the remaining CE concentration. Observed rate constants were determined. The reactions of TCE, cDCE, and tDCE were studied in a similar manner.

Catalyst Dependence Studies. Kinetic time courses were prepared as above with the [(TCPP)Co] varied from 80 to 800 nM for PCE degradation and from 180 to 1400 nM for TCE.

PCE Degradation. Titanium(III) Citrate Dependence Studies. Reaction vials were prepared with [(TCPP)Co] = 400 nM, and the reaction was initiated as described above. The titanium(III) citrate concentration was varied from 1.9 to 19.2 mM. Time points were collected at regular time intervals for the degradation of the first 10% of the PCE to observe the initial rate of dehalogenation. The initial reaction rates of PCE degradation were plotted against the titanium concentration.

PCE Degradation. pH Dependence. Kinetic profiles of dehalogenation reactions were prepared as above but in DI H_2O. The pH was adjusted from pH 5 to 9 with 1−150 μL spike additions of 5 M NaOH. The pH was measured before and after reductive dehalogenation by sacrificing vials.

Pairwise CE Competition Studies. PCE/cDCE degradation competition experiments were prepared as above with (TCPP)Co (9.44 μM) and initial PCE and cDCE concentrations of 54 and 65 μM, respectively. TCE/cDCE competition experiments were prepared with (TCPP)Co (9.44 μM) and initial TCE and cDCE concentrations of 81 and 84 μM, respectively.

Generation of Co^{I} Porphyrin Complexes. A variety of reducing agents were used to generate the Co^{I} oxidation state. The existence of the Co^{I} oxidation state was monitored with UV−vis absorbance spectroscopy at 364 and 411 nm for (TCPP)Co, (TPP)Co, and (MCPP)Co. Inner-sphere reducing agents, Ti^{III} and Cr^{II}, were used to generate the Co^{I} oxidation state ([cobalt porphyrin] = 7.5 μM, [Ti^{III}] = 0.8 mM, [Cr^{II}] = 2.3 mM) in H_2O, pH 8 (adjusted with aliquots of NaOH) and 2:1 *n*PrOH/H_2O (v/v). Additional reducing agents were also used in dried, degassed THF ([cobalt porphyrin] = 7.5 μM, [$LiAlH_4$(s)] = saturated in THF, [sodium benzophenone ketyl] = 0.43 mM). The Co^{I} porphyrin complex was reacted with benzyl bromide (50 μM) as a trap yielding Co^{III} complexes.

(Dichlorovinyl)(tetrakis(4-carboxyphenyl)porphyrin) Cobalt(III), (TCPP)Co(C_2HCl_2), 1. (TCPP)Co (2.1 mg, 2.5 μmol) dissolved in THF was reduced with sodium benzophenone ketyl (2 mL of 69 mM solution) dissolved in THF. The ketyl was prepared with 0.9 equiv of sodium metal (15.1 mg, 0.66 mmol) to favor the presence of the ketyl monoanion. The red porphyrin solution turned dark green upon treatment with the ketyl, and then TCE (0.5 mL, 5.62 mmol) was added. (−)-ESI-MS TOF (MeOH): m/z M^{2-} = 470.0 $[M]^-$ = 940.0.

(Dichlorovinyl)(tetraphenylporphyrin) Cobalt(III), (TPP)Co(C_2HCl_2), 2. A reaction sequence similar to the one above was followed. (TPP)Co (2.2 mg, 3.3 μmol) dissolved in THF was reduced with sodium benzophenone ketyl (2 mL of 69 mM solution) dissolved in THF. The red porphyrin solution turned dark green upon treatment with ketyl, and then TCE (0.5 mL, 5.62 mmol) was added. (+)-ESI-MS TOF (MeOH): m/z M^+ = 766.11, $[M + Na]^+$ = 789.10.

(*trans*-2-Chlorovinyl)(tetraphenylporphyrin) Cobalt(III), (TPP)Co(*trans*-C_2H_2Cl), 3. The methods of Sakurai and Setsune were followed for this preparation.[35,36] (TPP)CoCl (300 mg, 0.5 mmol) was prepared using the method of Sakurai with overnight stirring, and it was isolated in 72% yield. (TPP)Co(C_2H_2Cl) was prepared using Setsune's method. (TPP)CoCl (50 mg, 0.07 mmol) was dissolved in 20 mL of CH_2Cl_2 in a sealed flask and degassed by freeze−pump−thaw cycles. Acetylene (200 mL, 1 atm, 8.2 mmol) was added via vacuum transfer. The flask was sealed, thawed, and stirred overnight. Purification was performed by column chromatography (SiO_2, CH_2Cl_2) with a yield of 84%. X-ray quality crystals were obtained by slow evaporation from a hexane/CH_2Cl_2 (3:1) mixture. UV−vis (CH_2Cl_2): λ_{max} 409, 527 nm. ^{1}H NMR (CD_2Cl_2)

(35) Setsune, J.; Saito, Y.; Ishimaru, Y.; Ikeda, M.; Kitao, T. *Bull. Chem. Soc. Jpn.* **1992**, *65*, 639−648.
(36) Sakurai, T.; Yamamoto, K.; Naito, H.; Nakamoto, N. *Bull. Chem. Soc. Jpn.* **1976**, *49*, 3042−3046.

Table 2. Rate Constants of Chlorinated Ethylene Dehalogenation by (TCPP)Co

substrate	catalyst concn (μM)	k_{obs} ($\times 10^{-4}$ s^{-1})	k (M^{-1} s^{-1})	products (yield)	substrate one e$^-$ redox potential ($E°$, mV)[a]
PCE	0.68	1.69 ± 7	250	TCE (87%) cDCE (5%)	−0.598
TCE	0.91	0.22 ± 3	24	cDCE (84%) tDCE (4%) C_2H_2 (4%)	−0.674
cDCE	28	0.065 ± 0.4	0.24	C_2H_3Cl[b,c]	−0.955
tDCE	16	0.235 ± 0.1	1.5	C_2H_3Cl[b,d]	−1.012

[a] Calculated redox potentials vs SHE.[37] [b] The C_2H_3Cl yield was not determined, but its identity was verified with an authentic standard. [c] Isomerization to tDCE accounting for 33% of the cDCE loss was also observed. [d] Isomerization to cDCE accounting for 17% of the cDCE loss was also observed.

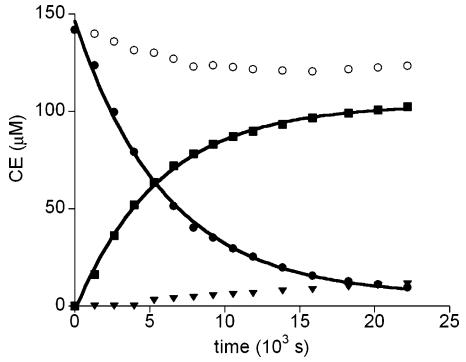

Figure 1. PCE degradation by 765 nM (TCPP)Co with the concurrent appearance of TCE and cDCE at 35 °C. [Ti^{III}] = 16 mM. PCE ●, TCE ■, cDCE ▼, mass balance ○. Curves are nonlinear first-order decay and growth fits to the data. No tDCE was observed.

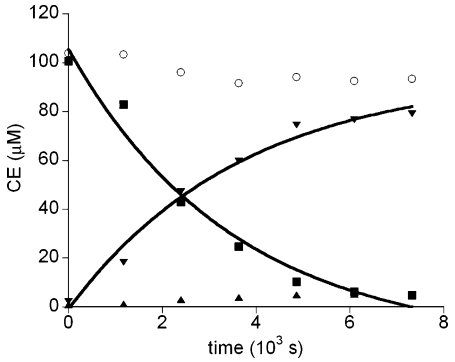

Figure 2. TCE degradation by 3.8 μM (TCPP)Co with the concurrent appearance of cDCE and other CEs at 35 °C. [Ti^{III}] = 16 mM. TCE ■, cDCE ▼, tDCE ▲, mass balance ○. Trace amounts of 1,1-DCE, vinyl chloride, acetylene, and ethylene were observed but not shown above. Curves are nonlinear first-order decay and growth fits yielding the observed rate constants for degradation and formation.

δ 8.91 (s, 8H), 8.12 (s, 8H), 7.75 (s, 12H), −0.40 (d, J = 11.7 Hz, 1H), −0.92 (d, J = 11.7 Hz, 1H). ^{13}C NMR (CD_2Cl_2) δ 145.4, 141.3, 133.6, 133.1, 128.0, 127.0, 122.1, 99.7. ESI-MS TOF (MeOH): m/z M^+ = 732.15, $[M + Na]^+$ = 755.13.

Results

CE Degradation Kinetics. The kinetics of the aqueous reductive dechlorination of PCE, TCE, cDCE, and tDCE catalyzed by (TCPP)Co were studied under pseudo-first-order conditions at pH 8 with titanium citrate as the bulk reducing agent. PCE and TCE were degraded under the reaction conditions, and the decay curves were well-fit to a single exponential over three half-lives indicating that the degradation of the chlorinated ethylene substrate was first order (Table 2). Because of the much slower dechlorination rates, the kinetic decays of cDCE and tDCE degradations were followed only for one to two half-lives (see Supporting Information). Because of this, the kinetic order is less certain for these substrates, but they also appear to follow first-order kinetics on the basis of fits to single exponential decays. During the control experiments, no dehalogenation was observed for any of the CE substrates in the absence of catalyst or bulk reductant.

PCE was rapidly degraded under the reaction conditions (1.69×10^{-4} s^{-1}, 680 nM catalyst, 35 °C). During PCE degradation, TCE was the major product (87%) with a small amount of cDCE (5%) also observed (Table 2). The mass balance for PCE degradation was determined from the concentrations of PCE, TCE, and cDCE (no tDCE detected) at each time point, and approximately 90% of the C_2 mass could be accounted for (Figure 1).

TCE degradation was found to occur an order of magnitude slower than the PCE degradation rate (2.2×10^{-5} s^{-1}, 910 nM catalyst, 35 °C). The major degradation product was cDCE (84%), and other observed products included tDCE (4%), 1,1-dichloroethylene (<1%), vinyl chloride (<1%), acetylene (4%), and ethylene (<1%) (Table 2). During dechlorination, a product selectivity of 21:1 for cDCE over tDCE was observed. The mass balance for TCE degradation was determined from the concentrations of TCE, cDCE, tDCE, and acetylene at each time point, and approximately 90% of the C_2 mass could be accounted for (Figure 2).

Both cDCE and tDCE are degraded considerably slower than PCE and TCE with cDCE being the most difficult to dechlorinate (cDCE, 6.5×10^{-6} s^{-1}, 28 μM catalyst, 35 °C; tDCE, 2.3×10^{-5} s^{-1}, 16 μM catalyst, 35 °C). In each case, the major degradation product was vinyl chloride. Isomerizations of cDCE and tDCE were observed during the dechlorination experiments. During cDCE degradation, the rate of isomerization of cDCE to tDCE was 33% of the overall cDCE degradation rate, determined by comparing the initial rates of degradation and formation. The rate of isomerization of tDCE to cDCE was found, in a similar manner, to be 17% of the overall tDCE degradation rate. No experiments were conducted to elucidate the isomerization mechanism.

Pairwise competition experiments (PCE/cDCE and TCE/cDCE) were carried out to further establish the faster degradation of the more chlorinated congener in the presence of its dehalogenation products and as a test for catalyst poisoning by product inhibition through the formation of an

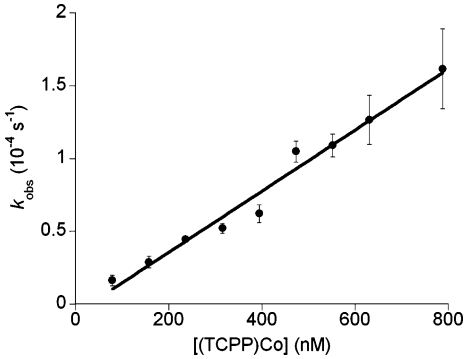

Figure 3. PCE degradation rate constant (k_{obs}) vs [(TCPP)Co]. The reactions were performed in pH 8 water at 35 °C. [Ti^{III}] = 16 mM. Error bars represent the standard error of the nonlinear fits to the data.

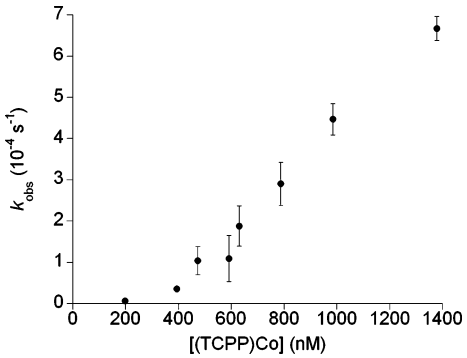

Figure 4. TCE degradation rate constant (k_{obs}) vs [(TCPP)Co]. The reactions were performed in pH 8 water at 35 °C. [Ti^{III}] = 16 mM. Error bars represent the standard error of the nonlinear fits to the data.

intermediate of low reactivity. During PCE degradation, no changes to the observed rate constants were observed in the presence of cDCE. For TCE, the presence of cDCE did not change the kinetics of TCE dehalogenation. Importantly, the presence of the slower reacting substrate did not inhibit the degradation of the faster one through catalyst poisoning.

The catalyst dependence of PCE and TCE degradation was determined by varying the catalyst concentration during degradation. For PCE, the concentration of (TCPP)Co was varied over the range of 80−800 nM. The observed rate constant varied linearly in response to (TCPP)Co concentration indicating a first-order dependence on the catalyst (Figure 3).

For TCE, the concentration of (TCPP)Co was varied over the range of 200−1400 nM. The observed rate constant varied linearly in response to (TCPP)Co concentration indicating a first-order dependence on catalyst (Figure 4).

We believe that the non-zero intercept may be the result of inhibition of the catalyst by an impurity. The nature of this impurity was pursued, and a TCE impurity, 1,1,2-trichloroethane, TCA, was identified with GC−MS. It was found to be present at 0.004% in TCE. While this concentration is too low to inhibit the (TCPP)Co-mediated TCE degradation at the level observed through the formation of a kinetically stable intermediate, experiments performed with both TCE (100 μM) and varying amounts of TCA (0, 7.0, and 70 μM) present showed that the TCE dehalogenation was inhibited by TCA (see Supporting Information).

Titanium(III) Citrate Dependence. The concentration of titanium(III) citrate was varied (1.9−19.2 mM), and the initial rates of PCE dechlorination were determined with 400 nM (TCPP)Co (Figure 5). At low concentrations, the rate increased linearly with bulk reductant concentration, but at high concentrations, saturation was observed. The trend line illustrates two zones of titanium dependence in the PCE degradation rate law: a linear first-order region and a saturation zero-order region.

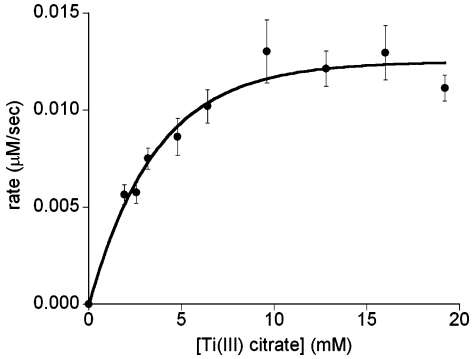

Figure 5. Initial rate of PCE degradation by (TCPP)Co (400 nM) during kinetic time courses in which the concentration of titanium(III) citrate was varied. Error bars represent the error determined from nonlinear fitting of the data.

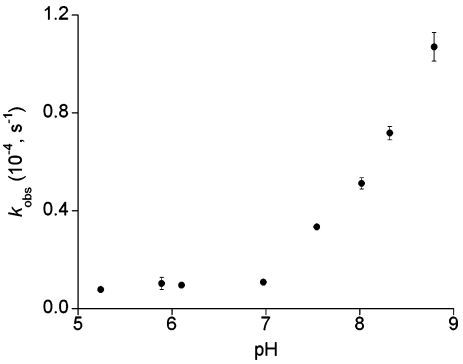

Figure 6. PCE degradation in DI water. [(TCPP)Co] = 770 nM and [Ti^{III}] = 16 mM, at 35 °C. The pH was adjusted with 1−150 μL additions of 5 M NaOH. The pH was measured before and after each reductive dehalogenation experiment. Error bars represent the standard error of the nonlinear fits to the data.

pH Dependence. As the pH was varied from 5 to 9, the observed rate constant of PCE dechlorination (770 nM (TCPP)Co) changed significantly. No dechlorination activity was observed below pH 7.0, but the observed rate constant increased linearly between pH 7 and 9 (Figure 6).

Generation and UV−Vis Characterization of Co^{I} Porphyrin Complexes. UV−vis absorbance spectroscopy was used to observe the cobalt oxidation state resulting from the interaction between (TCPP)Co^{II} and Ti^{III}. Cobalt porphyrin complexes have characteristic Soret band absorbance maxima for each oxidation state. The Co^{I} oxidation state is characterized by two bands in the Soret region with maxima at 364 and 411 nm and a reduced molar absorptivity coefficient relative to the Co^{II} and Co^{III} oxidation states.[38−40] In addition

(37) Totten, L. A.; Roberts, A. L. *Crit. Rev. Environ. Sci. Technol.* **2001**, *31*, 175−221.
(38) Kobayashi, H.; Hara, T.; Kaizu, Y. *Bull. Chem. Soc. Jpn.* **1972**, *45*, 2148−2155.
(39) Momenteau, M.; Fournier, M.; Rougee, M. *J. Chim. Phys. Phys.−Chim. Biol.* **1970**, *67*, 926−933.

Table 3. Reducing Agents and Cobalt(I) Absorbance Spectrum Observed

reducing agent[a]	solvent[b]	generation of Co^{I} [c] (TPP)Co	(TCPP)Co	(MCPP)Co
Ti^{III} citrate	H_2O, pH 8	*d*	yes	*d*
	2:1 *n*PrOH/H_2O, pH 8	no	yes	no
$(H_2O)_6$ Cr^{II}	H_2O, pH 8	*d*	yes	*d*
	2:1 *n*PrOH/H_2O, pH 8	no	yes	no
$LiAlH_4$	THF	yes	yes	yes
$Na^+Ph_2CO^-$	THF	yes	yes	yes

[a] [Ti^{III} citrate] = 0.8 mM; [$(H_2O)_6$ Cr^{II}] = 2.3 mM; [$LiAlH_4$] = saturated in THF; [$Na^+Ph_2CO^-$] = 0.43 mM. [b] All porphyrin complexes soluble at 7.5 μM unless otherwise indicated. [c] Based on appearance of bands at 364 and 411 nm. [d] Porphyrin complex not soluble.

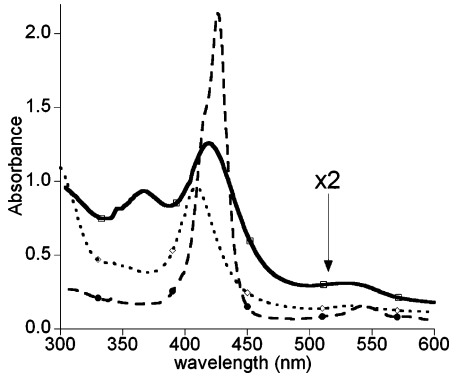

Figure 7. (TCPP)Co (7.5 μM) in H_2O at pH 8 treated with $Cr^{II}_{(aq)}$ and then benzyl bromide. Dashed line (TCPP)Co^{II} spectrum, solid line (TCPP)-Co^{I} spectrum (x2 absorbance values), and dotted line after addition of benzyl bromide.

to (TCPP)Co, the interactions between (TPP)Co and (MCP-P)Co and various reducing agents were compared for their ability to yield Co^{I} spectra for the three different cobalt porphyrin complexes.

Cobalt porphyrin solutions were prepared with 7.5 μM cobalt porphyrin in several solvents (H_2O pH 8, 2:1 *n*PrOH/H_2O (v/v) pH 8, and THF). (TPP)Co and (MCPP)Co were not soluble in water, but all of the cobalt porphyrin complexes were soluble in THF and 2:1 *n*PrOH/H_2O. A variety of reducing agents (titanium(III) citrate, aqueous chromous chloride, lithium aluminum hydride, and sodium benzophenone ketyl) were used to generate Co^{I} (Table 3). Solutions of the complexes were treated with the reducing agents, and the changes in the absorbance spectra were monitored (Figure 7). In the experiments that resulted in the appearance of the characteristic Co^{I} spectrum, the presence of Co^{I} was further verified through reaction with benzyl bromide (eq 1).[30,41−44] The change of the oxidation state to Co^{III} was monitored by changes in the absorbance spectrum.

$$(P)Co^{II} \xrightarrow[\text{agent}]{\text{reducing}} (P)Co^{I} \xrightarrow[\text{bromide}]{\text{benzyl}} (P)Co^{III}\text{-benzyl} \qquad (1)$$

Electrochemistry. Cyclic voltammetry was used to determine the Co^{I}/Co^{II} potential for the redox couples of (TCPP)Co, (MCPP)Co, and (TPP)Co with 0.5 mM cobalt complex in 0.1 M $TBAPF_6$ in DMF with a Ag/AgCl reference electrode. Cyclic voltammetry was used to determine the $E_{p,c}$ and $E_{p,a}$ for each complex (Table 4).

Table 4. Cyclic Voltammetry of the Cobalt Porphyrins Collected in 0.1 M [$n$$Bu_4N$][$PF_6$] DMF with a Ag/AgCl Reference Electrode

metal complex	$Co^{I/II}$ redox couple (mV)[a]	$Co^{I/II}$ redox couple (mV)[b]	ref
(TCPP)Co	−700	−745	this work
(TPP)Co	−695	−740	this work
		−870[c]	29
		−800[d]	45
(MCPP)Co	−680	−725	this work

[a] Referenced to the Ag/AgCl electrode. [b] Referenced to the SCE electrode. [c] DMF with $TBAClO_4$. [d] DMF with $TEAClO_4$.

Chlorovinyl Cobalt Porphyrin Complexes. Mass Spectrometric Observation of Dichlorovinyl Cobalt Complexes (TCPP)Co(C_2HCl_2) and (TPP)Co(C_2HCl_2). A dichlorovinyl cobalt porphyrin complex was observed in the reaction of in situ generated (TCPP)Co^{I} with TCE. The (TCPP)Co^{II} complex was dissolved in THF and reduced with sodium benzophenone ketyl, and the intensity of the color diminished. Then, 3 drops of pyridine were added, followed by 500 μL of neat TCE (eq 2). An immediate color change, to a brown-green solution, upon addition of TCE was observed.

$$(TCPP)Co^{II} \xrightarrow[\text{THF}]{Na^+Ph_2CO^-} (TCPP)Co^{I} \xrightarrow[\text{THF, py}]{\text{TCE}} (TCPP)Co^{III}(C_2HCl_2) \qquad (2)$$

The analysis of the reaction products with negative mode electrospray ionization ((−)-ESI-TOF) mass spectrometry indicated masses for M^- and M^{2-} (940.0 and 470.0 *m*/*z*, respectively) for a (TCPP)Co(C_2HCl_2) complex, **1**, and the signals exhibited an isotope pattern indicative of the incorporation of two chlorine atoms (high-resolution mass spectrometry (HRMS) was unsuccessful).

In a similar manner, (TPP)Co was treated with the same reaction conditions, and the products were analyzed with (+)-ESI-TOF. The observed masses for M^+ and $[M + Na]^+$ (766.11 and 789.10 *m*/*z*, respectively) were consistent with those of (TPP)Co(C_2HCl_2), **2**. The isotope patterns were consistent with two chlorine atoms being incorporated into the products. The composition of (TPP)Co(C_2HCl_2) was confirmed with ESI-TOF HRMS by comparison to a propylene glycol 1000 (1000 PPG) standard.

Preparation of (TPP)Co(*trans*-C_2H_2Cl). The (TPP)CoCl complex was prepared by the method of Sakurai,[36] and (TPP)Co(*trans*-C_2H_2Cl), **3**, was prepared from the chloro complex following the method of Setsune[35] (eq 3). It was isolated in a 60% overall yield.

$$(TPP)Co^{II} \xrightarrow[\text{MeOH, rt}]{\text{HCl concd}} (TPP)Co^{III}Cl \xrightarrow[CH_2Cl_2\text{, rt}]{C_2H_2} (TPP)Co^{III}(C_2H_2Cl) \qquad (3)$$

(40) Whitlock, H. W., Jr.; Bower, B. K. *Tetrahedron Lett.* **1965**, 4827−4831.
(41) Fukuzumi, S.; Maruta, J. *Inorg. Chim. Acta* **1994**, *226*, 145−150.
(42) Maiya, G. B.; Han, B. C.; Kadish, K. M. *Langmuir* **1989**, *5*, 645−650.
(43) Zeng, Z.; Jewsbury, R. A. *Analyst* **1998**, *123*, 2845−2850.
(44) Zhou, D. L.; Walder, P.; Scheffold, R.; Walder, L. *Helv. Chim. Acta* **1992**, *75*, 995−1011.

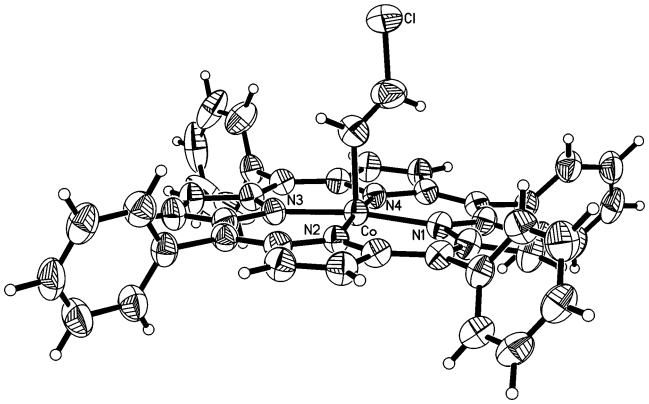

Figure 8. X-ray structure of (TPP)Co(*trans*-C_2H_2Cl) with thermal ellipsoids drawn at the 50% probability level.

Scheme 2. Simple Proposed Catalytic Cycle for the (TCPP)Co-Mediated Reductive Dechlorination of Chlorinated Ethylenes, Exemplified by the Conversion of TCE to cDCE

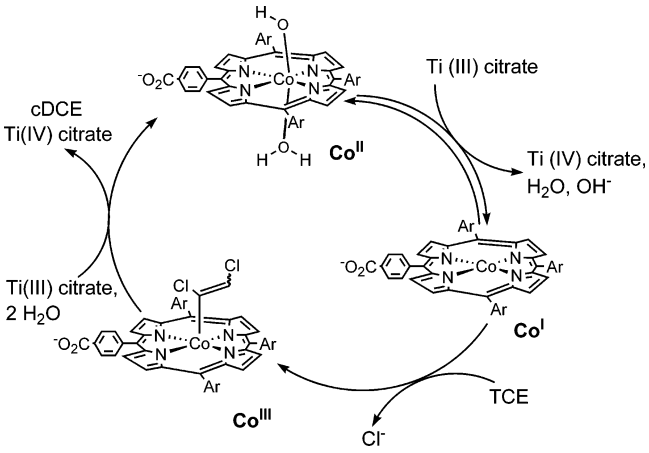

An absorbance spectrum was collected in CH_2Cl_2 of the purified material with λ_{max} values of 409 and 527 nm, which agrees with the reported data.[35] The ^{1}H NMR chemical shift of the vinyl protons is notable because they are significantly shielded upfield to δ −0.40 and −0.92 and have a coupling constant of 11.7 Hz, which is slightly smaller than the normal 12−18 Hz range for *trans*-alkenyl protons, but consistent with the reported spectrum.[35] The composition was confirmed with (+)-ESI-TOF HRMS by comparison to the standard. X-ray quality crystals were obtained by slow evaporation from a 3:1 mixture of hexanes and CH_2Cl_2. The structure is shown in Figure 8 and confirms the *trans*-chlorovinyl confirmation. (See Supporting Information for crystallographic data.) The cobalt atom is 0.123 Å above the N_4 porphyrin plane, showing little distortion from planarity. The Co−N distances are equal and are consistent with other Co porphyrin structures. The Co−C bond distance (1.926 Å) is slightly shorter than those of other chlorovinyl cobalt complexes.[21−24] (See Supporting Information.)

Discussion

Simplified Catalytic Cycle. We propose the simplified catalytic cycle for (TCPP)Co degradation of CEs shown in Scheme 2 on the basis of these experimental results and the catalytic cycle for vitamin B_{12}-mediated reductive dehalogenation.[13−15,20,22,23] From the work of Pasternack and the pH during dehalogenation, we propose that (TCPP)Co^{II} should be coordinated with a hydroxo and an aquo ligand prior to reduction.[46] As established by the UV−vis experiments, the reduction of (TCPP)Co^{II} by Ti^{III} citrate yields (TCPP)Co^{I}, which is critical to CE dehalogenation because no degradation was observed in controls without Ti^{III} citrate. On the basis of solution studies and the solid-state structure of (TPP)Co^{I}, the cobalt(I) oxidation state should be free of axial ligands.[29,38,47,48] The mass spectrometry results from the reaction of (TCPP)Co^{I} or (TPP)Co^{I} with TCE and the isolation and single-crystal structure of (TPP)Co(*trans*-C_2H_2-Cl) give evidence for the intermediacy of chlorovinyl cobalt complexes.

The B_{12} and (TCPP)Co systems share a number of similarities that suggest they may operate by the same mechanisms. Most notably, the two systems degrade PCE and TCE through the sequential replacement of chlorine atoms by hydrogen atoms with the same empirical rate laws. Both systems display higher degradation rate constants for the more chlorinated congeners. In addition, the importance of the Co^{I} oxidation state to the vitamin B_{12}[14,20] and (TCPP)Co systems and the preparation of chlorovinyl cobalt complexes are further indications of shared mechanisms.

(TCPP)Co is a highly active aqueous-phase dechlorination catalyst which works against CEs. Degradation rate laws for PCE (eq 4) and TCE (eq 5), based on the kinetic data, are first order in both catalyst and CE substrate.

$$\frac{-\mathrm{d[PCE]}}{\mathrm{d}t} = k\mathrm{[PCE][(TCPP)Co]} \quad (4)$$

$$\frac{-\mathrm{d[TCE]}}{\mathrm{d}t} = k\mathrm{[TCE][(TCPP)Co]} \quad (5)$$

Comparison of the dechlorination bimolecular rate constants of B_{12} to our (TCPP)Co results yields a dechlorination enhancement of 5.6 and 14 times for PCE and TCE, respectively, over B_{12} (Table 5).

During TCE degradation, both vitamin B_{12} and (TCPP)-Co yielded a decisive product selectivity for cDCE over tDCE. For (TCPP)Co, a 21:1 selectivity of cDCE over the tDCE isomer was observed, while for B_{12}, there was a 23:1 selectivity for the cis isomer. For B_{12}, this selectivity has

Table 5. Comparison of Vitamin B_{12} and (TCPP)Co Bimolecular Rate Constants

substrate	B_{12} k (M^{-1} s^{-1})[a]	(TCPP)Co k (M^{-1} s^{-1})	k((TCPP)Co)/k(B_{12})
PCE	44.1	250	5.6
TCE	1.69	24	14
cDCE	0.01	0.24	24
tDCE	0.03	1.5	50

[a] Reaction conditions: 46 μM vitamin B_{12}, 27 mM titanium(III) citrate, 2.2 mM CE substrate, pH 8.2, 22 °C.[13]

(45) Giraudeau, A.; Callot, H. J.; Jordan, J.; Ezhar, I.; Gross, M. *J. Am. Chem. Soc.* **1979**, *101*, 3857−3862.
(46) Pasternack, R. F.; Parr, G. R. *Inorg. Chem.* **1976**, *15*, 3087−3093.
(47) Doppelt, P.; Fischer, J.; Weiss, R. *Inorg. Chem.* **1984**, *23*, 2958−2962.
(48) Kellett, R. M.; Spiro, T. G. *Inorg. Chem.* **1985**, *24*, 2373−2377.

been explored with CEs[13,14,49] and CE analogues[20] and has been regularly observed. This selectivity appears to be the result of the formation of (*E*)-dichlorovinyl cobalt complexes[23,24] as catalytic cycle intermediates, and this is a likely cause in the (TCPP)Co system as well.

An interesting finding for TCE degradation was the observation that TCA inhibits the degradation. This fact combined with the non-zero intercept of the dependence of the TCE dechlorination rate on catalyst concentration (Figure 4) suggested that TCA contamination might be responsible for the apparent inhibition at catalyst concentrations below 200 nM. However, the TCA impurity concentration is too low (4 nM TCA in a 100 μM TCE solution) to fully account for the inhibition observed, and TCA does not appear to be a potent inhibitor. The apparent lack of catalyst activity at concentrations below 200 nM may be a result of inhibition by an as yet unidentified species. Nevertheless, the fact that TCA can act as an inhibitor at higher concentrations raises concerns about the use of (TCPP)Co for remediation of sites with a mixture of chlorinated ethenes and ethanes.

The slow degradation of cDCE by (TCPP)Co could be caused by either the slow initial reaction between (TCPP)-Co^{I} and cDCE or the slow regeneration of the active catalyst species through the formation of stable intermediates that deactivate a portion of the catalyst. By stable intermediates, we mean species formed that are effectively unreactive over the course of hours (the time scale of our experiments) under the catalytic conditions employed and, thus, represent catalytically inactive cobalt porphyrin species. To test this, PCE degradation was performed in the presence of cDCE and compared to control experiments without cDCE. Similarly, TCE degradation was performed in the presence of cDCE. Inhibition was not observed in either case, indicating that the slow catalytic degradation of cDCE likely results from the slow reaction between (TCPP)Co^{I} and cDCE and not the formation of a kinetically stable porphyrin complex that slows or prevents catalyst turnover.

Titanium Dependence. Varying the titanium(III) citrate concentration had a strong effect on the initial rates of PCE dehalogenation. At a low reductant concentration, a linear relationship between increasing [Ti^{III}] and rate was observed suggesting a first-order dependence of the rate-limiting step upon the bulk reductant. However, at higher Ti^{III} concentrations, saturation was reached indicating no bulk reductant dependence. The degradation of PCE can be represented as the sum of two processes: catalyst activation (eq 6) and reaction with CE substrate (eq 7).

$$(\text{TCPP})\text{Co}^{\text{II}} + \text{Ti}^{\text{III}} \underset{k_{-1}}{\overset{k_1}{\rightleftharpoons}} (\text{TCPP})\text{Co}^{\text{I}} + \text{Ti}^{\text{IV}} \qquad (6)$$

$$(\text{TCPP})\text{Co}^{\text{I}} + \text{PCE} \xrightarrow{k_2} (\text{TCPP})\text{Co}^{\text{II}} + \text{products} \qquad (7)$$

Reduction of (TCPP)Co^{II} to (TCPP)Co^{I} occurs, despite the fact that (TCPP)Co^{I} is a stronger reductant than Ti(III) citrate, by virtue of the large excess of Ti^{III}. In a typical experiment, the Co/Ti ratio is 1:40 000 (400 nM (TCPP)Co^{II} and 16 mM Ti^{III} citrate), and even at this ratio, the calculated conversion of (TCPP)Co^{II} to (TCPP)Co^{I} is only 70% (see Supporting Information). The saturation behavior in the Ti^{III} citrate dependence is consistent with competitive destruction of (TCPP)Co^{I} by reaction with PCE. Application of the steady-state approximation for (TCPP)Co^{I} (eq 8) to the mechanism outlined in eqs 6 and 7 gives the rate law shown in eq 9 where $[\text{Co}]_T \approx [\text{Co}^{\text{I}}] + [\text{Co}^{\text{II}}]$.

$$[\text{Co}^{\text{I}}] = \frac{k_1[\text{Co}^{\text{II}}][\text{Ti}^{\text{III}}]}{k_{-1}[\text{Ti}^{\text{IV}}] + k_2[\text{PCE}]} \qquad (8)$$

$$\frac{\text{d}[\text{PCE}]}{\text{d}t} = -\frac{k_2 \frac{k_1}{k_{-1}} \frac{[\text{Ti}^{\text{III}}]}{[\text{Ti}^{\text{IV}}]}[\text{Co}]_T\,[\text{PCE}]}{1 + \frac{k_1}{k_{-1}} \frac{[\text{Ti}^{\text{III}}]}{[\text{Ti}^{\text{IV}}]} + \frac{k_2}{k_{-1}}[\text{PCE}]} \qquad (9)$$

Under our experimental conditions ([PCE] $\leq$ 100 μM), k_2/k_{-1}[PCE] $\ll$ 1 which allows us to simplify the rate law (eq 10).

$$\frac{\text{d}[\text{PCE}]}{\text{d}t} = -\frac{k_2 \frac{k_1}{k_{-1}} \frac{[\text{Ti}^{\text{III}}]}{[\text{Ti}^{\text{IV}}]}[\text{Co}]_T[\text{PCE}]}{1 + \frac{k_1}{k_{-1}} \frac{[\text{Ti}^{\text{III}}]}{[\text{Ti}^{\text{IV}}]}} = k_{\text{obs}}[\text{PCE}] \qquad (10)$$

The low and high [Ti^{III}] limits are given in eqs 11 and 12.

$$k_{\text{obs}} = k_2 \frac{k_1}{k_{-1}} \frac{[\text{Ti}^{\text{III}}]}{[\text{Ti}^{\text{IV}}]}[\text{Co}]_T;\ \frac{k_1}{k_{-1}} \frac{[\text{Ti}^{\text{III}}]}{[\text{Ti}^{\text{IV}}]} \ll 1 \qquad (11)$$

$$k_{\text{obs}} = k_2[\text{Co}]_T;\ \frac{k_1}{k_{-1}} \frac{[\text{Ti}^{\text{III}}]}{[\text{Ti}^{\text{IV}}]} \gg 1 \qquad (12)$$

We believe that the simple kinetic model satisfactorily explains the Ti^{III} dependence on the reaction kinetics and indicates that the most favorable condition for PCE degradations is when the Ti/Co ratio is high enough to be near the saturated rate limit (>20 000:1).

pH Dependence. The pH of the reaction conditions has a significant effect on the degradation kinetics and on the chemical properties of the constituents of this system (i.e., the titanium(III) citrate reduction potential, (TCPP)Co aqueous solubility, and the protonation state of the catalyst). The titanium reduction potential varies with pH; at pH 7 the reduction potential is -480 mV, and it varies linearly (-60 mV/pH) from pH 7 to 9.[15,50] As a result, the pH data can be interpreted with an electrochemical analysis based on the redox couples of titanium citrate and (TCPP)Co and their concentrations (Figure 9 and see Supporting Information).

However, the pH versus degradation data may reflect a preference for a specific protonation state of the catalyst during the reduction. On the basis of the pH of the dechlorination reaction conditions, the (TCPP)Co protonation state in Scheme 2 is suggested by the following data. (TCPP)-Co has sparing aqueous solubility in strongly acidic solutions

(49) Follett, A. D.; McNeill, K. *J. Am. Chem. Soc.* **2005**, *127*, 844−845.

(50) Zehnder, A. J. B.; Wuhrmann, K. *Science* **1976**, *194*, 1165−1166.

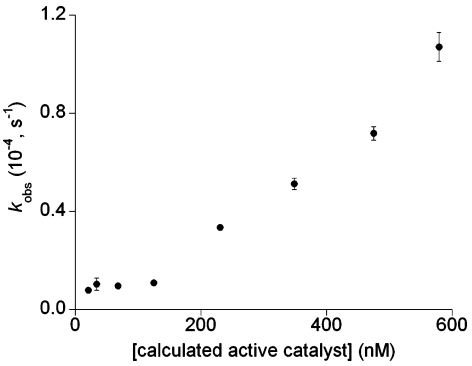

Figure 9. pH dependent active catalyst concentration vs PCE degradation, k_{obs} ([(TCPP)Co]$_{tot}$ = 770 nM, [Ti^{III}] = 16 mM, 35 °C), as determined by electrochemical data and species concentrations. Data points represent individual kinetic profiles at different pH values, and error bars are the error in the least-squares fitting of the degradation data.

but is readily soluble in alkaline solutions (see Supporting Information). This effect is likely due to the pK_a values of (TCPP)Co, which can be estimated or are known. If the carboxyphenyl moieties are similar to the substituted benzoic acids, the pK_a values would be ~4.2. Two cobalt-coordinated water molecules have pK_a values of 7.5 and 9.0.[46] Thus, between pH 4 and 7, predominantly peripheral deprotonation of the carboxylic acids takes place. Yet, under those conditions, no dehalogenation activity was observed. The fractional composition of a complex with at least one deprotonated coordinating waters increases above approximately pH 7.0 and dehalogenation is observed (see Supporting Information).

With (TCPP)Co in aqueous solution at pH 8, two types of binding are available for coordinating a reduced metal center (e.g., Ti^{III} or Cr^{II}) through the peripheral carboxylates and the metal-bound hydroxo/aquo ligands. Arguments for[51] and against[52] the involvement of the peripheral moieties, such as the carboxylates of TCPP complexes, in electron-transfer reactions have been put forth. There are significant precedents for OH and other groups to act as bridging ligands for electron transfer with Ti^{III} and Cr^{II} as the reducing agents.[51−56] We, currently, do not favor an inner-sphere pathway involving the peripheral carboxylates. Evidence against a peripheral inner-sphere mechanism comes from the pH dependence data (where no dehalogenation was observed despite the presence of free carboxylates) and dehalogenation experiments using Cr^{II} as the bulk electron source. With a peripheral pathway, we expected, because of the formation of kinetically inert Cr^{III} carboxylate complexes, that at most four turnovers would be possible in this system; more than 10 turnovers were observed (see Supporting Information).

Co(I) as the Active Oxidation State. In an effort to elucidate the active dehalogenation oxidation state and the preferred cobalt reduction pathway, we subjected (TCPP)Co, (TPP)Co, and (MCPP)Co to the reducing environment of the degradation conditions. (TPP)Co and (MCPP)Co were used because of the differences between their functional groups and those of (TCPP)Co. In aqueous solvent mixtures, (TCPP)Co was more amenable to reduction to Co^{I} with Ti^{III} or Cr^{II} than either (TPP)Co or (MCPP)Co. Yet in THF with powerful reducing agents, $LiAlH_4$ and $NaPh_2CO$, spectroscopic evidence of Co^{I} generation was obtained for all cobalt porphyrins. The differences in reducibility between (TCPP)Co and the other cobalt porphyrin complexes is not a result of differences in redox potential. As has been reported, meso substitution of cobalt porphyrins has a negligible effect on the redox couple of the metal center.[28,58] This observation is also supported by our electrochemical measurements. Even though there are essentially no electrochemical differences among (TPP)Co, (MCPP)Co, and (TCPP)Co, the latter is more readily reduced, indicating that the carboxylic acid groups do have some as yet undetermined effect on facilitating reduction.

Chlorovinyl Cobalt Porphyrin Complexes. There is a growing body of evidence that implicates chlorovinyl complexes as intermediates in the catalyzed dechlorination of CEs by B_{12} through their observation and synthesis for the native catalyst and with model complexes.[14,22−24,63] We have obtained evidence for such complexes as intermediates in this system through the reaction of in situ generated Co^{I} and TCE yielding **1** and **2** and the preparation of **3**. The preparation of **3** and its stability indicate that isolation and characterization of the dichlorovinyl cobalt complexes (**1** and **2**) may be possible, and such work is ongoing.

Conclusions

A highly active dechlorination catalyst has been identified, and its kinetic activity has been characterized under a variety of conditions. While similar in its dehalogenation behavior, (TCPP)Co is kinetically superior to vitamin B_{12}. The dechlorination is sensitive to pH and shows heightened activity in response to increasing concentrations of titanium citrate. Mass spectrometric evidence for chlorovinyl cobalt porphyrin complexes as catalytic cycle intermediates has been obtained, and a chlorovinyl model complex of (TPP)Co has been prepared and structurally characterized.

Acknowledgment. This work was funded in part by the EPA STAR Fellowship program (Grant U-91610701-1) and the National Science Foundation (Grant CHE-0239461). We thank Victor G. Young, Jr., and the X-ray Crystallographic Laboratory for help in solving the (TPP)Co(*trans*-C_2H_2Cl) structure.

(51) Fleischer, E. B.; Cheung, S. K. *J. Am. Chem. Soc.* **1976**, *98*, 8381−8387.
(52) Balahura, R. J.; Trivedi, C. P. *Inorg. Chem.* **1978**, *17*, 3130−3132.
(53) Pasternack, R. F.; Sutin, N. *Inorg. Chem.* **1974**, *13*, 1956−1960.
(54) Balahura, R. J.; Johnston, A. *Inorg. Chem.* **1986**, *25*, 652−656.
(55) Hery, M.; Wieghardt, K. *Inorg. Chem.* **1978**, *17*, 1130−1134.
(56) Bertram, H.; Wieghardt, K. *Inorg. Chem.* **1979**, *18*, 1799−1807.
(57) Zheng, G.; Stradiotto, M.; Li, L. *J. Electroanal. Chem.* **1998**, *453*, 79−88.
(58) Kadish, K. M.; Morrison, M. M. *Bioinorg. Chem.* **1977**, *7*, 107−115.
(59) Kadish, K. M.; Bottomley, L. A.; Kelly, S.; Schaeper, D.; Shiue, L. R. *Bioelectrochem. Bioenerg.* **1981**, *8*, 213−222.
(60) Kadish, K. M.; Morrison, M. M. *Bioelectrochem. Bioenerg.* **1976**, *3*, 480−490.
(61) Kadish, K. M. *Prog. Inorg. Chem.* **1986**, *34*, 435−605.
(62) Kadish, K. M.; Lin, X. Q.; Han, B. C. *Inorg. Chem.* **1987**, *26*, 4161−4167.
(63) Lesage, S.; Brown, S.; Millar, K. *Environ. Sci. Technol.* **1998**, *32*, 2264−2272.

Supporting Information Available: cDCE and tDCE degradation kinetic profiles, calculated active catalyst concentration as a function of pH, electrochemical data, and (TPP)Co(*trans*-C_2H_2Cl) crystallographic information. This material is available free of charge via the Internet at http://pubs.acs.org.

IC0504339